DOI: 10.61782/fa.2025.0880

THE RELATIONSHIP BETWEEN DAMAGE RISK CRITERIA FOR IMPULSE NOISE EXPLAINED BY SIMPLE ACOUSTICAL DESCRIPTORS

Marian Weger*
French-German Research Institute of Saint-Louis (ISL), Saint-Louis, France

ABSTRACT

Hazardous impulse noise is still a major problem for personnel in industry and construction work, and particularly in the military. The allowed maximum permissible exposures per day for a certain combination of noise and hearing protection differ across countries, depending on the applicable criterion for predicting auditory hazard. Such Damage Risk Criteria (DRC) for impulse noise may take into account signal extrema, zero-crossings, amplitude/energy statistics, or physical ear models. Consequently their reactions to environmental and source characteristics diverge. We evaluated the differences between DRC and their correlations with acoustical descriptors. Most of the variance between hazard predictions by DRC could be explained by linear regression using only a few descriptors that cover certain key sound characteristics or peculiarities of the hearing system. This relationship allows us to better understand how certain sound characteristics translate to the risk of hearing damage and contributes to the ongoing discussion on future DRC standards. As the data comprised only a subset of soldiers' noise exposure, follow-up studies should include larger caliber weapons and complex noise combined with hearing protection, in order to draw more general conclusions.

Keywords: *impulse noise, damage risk criteria, weapon noise, auditory hazard, hearing injury*

1. INTRODUCTION

Despite all efforts and advances in noise control and Hearing Protection Devices (HPD), loud impulse noise still constitutes a major health risk for personnel in industry, construction work, and within the military. Especially during military training, noise exposures from firearms can induce hearing injury among soldiers. In order to quantify a soldier's individual risk of hearing injury, several objective Damage Risk Criteria (DRC) have been proposed. Their predictions, however, diverge, especially for ecologically valid scenarios comprising both continuous noise (from vehicles) and impulse noise (from weapon systems). Even within the EU, several national standards are in use; e.g., Pfander criterion in Germany, LAeq in France, or the Auditory Hazard Assessment Algorithm for Humans (AHAAH) in The Netherlands, and also the thresholds for the maximum admissible daily noise dose vary. At the time of writing, no currently available standard is sufficiently validated in order to cover all relevant aspects of auditory hazard. In addition, the differences between DRC as well as their individual qualities and restrictions are not yet entirely understood. The topic is therefore still subject to extensive civilian and military research worldwide. Various studies have compared existing DRC against each other, with respect to the predicted hazard or the resulting Maximum Permissible Exposures (MPE) per day (and per weapon/HPD combination).

For example, van der Eerden et al. [1] compared the A-weighted Sound Exposure Level (ASEL) to the risk predicted by the AHAAH. They concluded that there is no simple correlation between the two, especially due to the AHAAH's non-monotonic behavior. In particular, with growing impulse strength in terms of increasing Weber radius of synthesized Friedlander waves, ASEL grows monotonically, while the hazard predicted by the AHAAH decreases again, after having reached its maximum at an ASEL of around 140 dBA. In addition, the authors found that the AHAAH was disproportionately sensitive to additive continuous noise in comparison to ASEL. This can also be interpreted as low robustness against SNR [2].

***Corresponding author**: *marian.weger@isl.eu.*

The Pfander criterion ignores any sound below -10 dB with respect to the peak [3]. A major difference between Pfander and AHAAH thus concerns the inclusion of room reflections. Furthermore, their relationship shows the same non-monotonic behavior as between ASEL and AHAAH [3]. Pfander and ASEL were assumed to be too different to be converted into one another [4].

As ASEL also covers continuous noise, it is widely used in any context. For complex noise that exhibits both impulsive and continuous components, however, an adjustment in terms of "impulsiveness" (quantified by statistical kurtosis) correlated better with medical data than ASEL alone [5]. Likewise, the US military standard 1474E [6] includes an adjustment by the duration of the impulse in order to correct ASEL's assumed overestimation of large-caliber weapon noises.

As most of the mentioned studies were based on synthesized sounds, they provide valuable insights into the direct relationship between DRC and certain controlled parameters. However, these results cannot be easily transferred to actual weapon usage under realistic training conditions. We therefore compared hazard predictions by several DRC based on real recordings of shooting noise with different weapon configurations and under different ecologically valid environmental conditions (indoor and outdoor). The dataset is briefly described in Sec. 2, while the evaluated DRC are summarized in Sec. 3.

We further tried to predict the differences between DRC by selected acoustical descriptors that are supposed to cover sound qualities which might cause the respective differences. These descriptors are summarized in Sec. 4. In Sec. 5, correlations between DRC are analyzed and discussed in terms of their prediction by acoustical descriptors using multiple linear regression. Finally, general conclusions are drawn in Sec. 6.

2. DATASET & PREPROCESSING

The evaluation is based on the same dataset as described in [2]. It comprises impulsive noise events that were recorded within the multinational measurement campaign NATO RTG SET-286 carried out in 2023. These included 10 single shots with 9 weapon configurations reaching from pistol to anti-material rifle (some with silencer) using live ammunition in 8 environmental conditions (4 outdoor, 4 indoor) as well as 4 explosive configurations (stun grenade and 3 different door breaching charges) with 4 repetitions. Cleaned from defective items, the dataset includes 731 impulses. The stimuli are assumed to cover a majority of infantry soldiers' noise exposure. Recordings were made in 1 m distance at $90°$ left to the muzzle, with respect to shooting direction, at 1.6 m height or approximate ear level (for explosive, distances were only approximate between 1 m and 3 m).

For the calibrated recordings, the phase was occasionally flipped to always positive peak, DC offset was removed, and noise events were cut to 1 s duration, with the onset (where the amplitude first reaches -3 dB resp. peak) aligned to 5 ms. Signals were low-pass filtered by an 8th-order Bessel filter at 22 kHz cutoff frequency, as recommended by [7].

3. DAMAGE RISK CRITERIA

For each noise event of the above-described dataset, the auditory hazard was predicted by 6 different DRC: Pfander, Leq, LAeq, LIAeq, LAeq-Kurtosis, and AHAAH. Irrespective of the applicable limit, each of these DRC includes a hazard prediction function that we express in the form of hazard level L_{H} in dB for allowing meaningful comparisons. As the exact definitions used in this work may differ from other publications or national standards, we briefly summarize them below.

The Pfander criterion expresses auditory hazard by the Pfander level $L_{\mathrm{H}}^{\mathrm{Pfander}}$, see Eqn. (1), which depends on the unweighted (or Z-weighted) peak Sound Pressure Level (SPL) $\hat{L}_{\mathrm{p}}$ and C-duration T_{C} which is the sum of all time periods during which the waveform exceeds -10 dB below $\hat{L}_{\mathrm{p}}$ [8].

$$L_{\mathrm{H}}^{\mathrm{Pfander}} = \hat{L}_{\mathrm{p}} + 10\log_{10}\left(T_{\mathrm{C}}\right) \quad (1)$$

Leq predicts hazard based on sound energy. Sound exposure within a certain period of time is $E = \int p(t)^2 \mathrm{d}t$. The unweighted Sound Exposure Level (SEL) or L_{E} with respect to $E_0 = 400\,\mu\mathrm{Pa}^2\mathrm{s}$ is then interpreted as hazard level $L_{\mathrm{H}}^{\mathrm{SEL}}$:

$$L_{\mathrm{H}}^{\mathrm{Leq}} = \mathrm{SEL} = L_{\mathrm{E}} = 10\log_{10}\left(E/E_0\right) \quad (2)$$

LAeq extends Leq by incorporating the A-weighted sound exposure E_{A}:

$$L_{\mathrm{H}}^{\mathrm{LAeq}} = \mathrm{ASEL} = L_{\mathrm{A,E}} = 10\log_{10}\left(E_{\mathrm{A}}/E_0\right) \quad (3)$$

LIAeq is an extension to LAeq that adjusts ASEL through the A-duration T_{A}, i.e., the duration between the last zero crossing before and the first zero crossing after the peak, as given in Eqn. (4). In the actual standard, T_{A} is restricted between 0.2 ms and 2.5 ms [6]; however, as no other DRC includes such hard parameter clipping, we leave T_A unrestricted for the current evaluation. Note that we use the alternative version for 1 s window length [6].

$$L_\mathrm{H}^\mathrm{LIAeq} = L_\mathrm{A,E} - 1.5 \cdot 10 \log_{10}\left(T_\mathrm{A}/0.2\,\mathrm{ms}\right) \quad (4)$$

LAeq-Kurtosis, originally developed for complex factory noise [9], adjusts ASEL by the statistical measure of kurtosis β, as given in Eqn. (5). A $\beta > 3$ (larger than kurtosis of Gaussian noise) means stronger tails of the probability distribution, i.e., more extreme values due to impulses. The amount of adjustment is set to $\lambda = 4.02$ [9]. Kurtosis is computed for the entire 1 s analysis window.

$$L_\mathrm{H}^\mathrm{LAeq\text{-}K} = L_\mathrm{A,E} + \lambda \log_{10}\left(\beta/3\right) \quad (5)$$

The AHAAH implements a physical model of the hearing system. It interprets the maximum basilar membrane displacement due to noise exposure as potential hazard H^AHA, expressed in Auditory Risk Units (ARU) and hazard level after (6). Note that we consider only the unwarned mode, meaning that the acoustic reflex is initially deactivated and gets triggered by the impulse [10, 3]. The acoustic reflex ramps in with a time constant of $\tau = 11.7\,\mathrm{ms}$, starting at 9 ms after the 134 dB threshold is exceeded for the first time. For consistent results with lower levels, we use an adaptive threshold at -3 dB below the peak. Due to the sharp rising edge of weapon noises, in theory following a Friedlander wave, the resulting error in trigger time is considered negligible.

$$L_\mathrm{H}^\mathrm{AHA} = 10 \log_{10}\left(H^\mathrm{AHA}/10^{-10}\,\mathrm{ARU}\right) \quad (6)$$

4. ACOUSTICAL DESCRIPTORS

In order to better understand the differences between DRC, we tried to predict their results by different combinations of acoustical descriptors. These are briefly summarized below.

4.1 Peak, action times, and energy

Most of the examined DRC themselves are already constructed from a couple of descriptors which we include into the analysis: peak SPL $\hat{L}_\mathrm{p}$, C-duration T_C, A-duration T_A, SEL L_E, ASEL $L_\mathrm{A,E}$, kurtosis k. In addition to these, we add common variants using A- and C-weighting that are not yet contained: $\hat{L}_\mathrm{A,p}$, $\hat{L}_\mathrm{C,p}$, and CSEL ($L_\mathrm{C,E}$) To account for spectral differences, we use the Spectral Centroid (SC) that is the frequency-weighted sum of spectral bins normalized by their unweighted sum.

4.2 Diffuseness

An important sound characteristic that is not yet covered by the above descriptors is diffuseness, i.e., the amount of reflections or reverberation that is defined by the environment in which the noise is perceived. A simple statistical descriptor for diffuseness is the Direct-to-Reverberant energy Ratio (DRR), i.e., the ratio between direct and reverberant sound energy. In practice, a Room Impulse Response (RIR) is split at an arbitrary time, typically 2.5 ms after the onset, into the direct and the reverberant part. For impulse noise, the recordings can already be interpreted as impulse responses, which allows us to directly obtain DRR according to Eqn. (7):

$$\mathrm{DRR} = 10 \log_{10}\left(\frac{\int_{t=0}^{2.5\,\mathrm{ms}} p(t)^2 \mathrm{d}t}{\int_{t=2.5\,\mathrm{ms}}^{\infty} p(t)^2 \mathrm{d}t}\right) \quad (7)$$

4.3 Psychoacoustical descriptors

If the frequency weighting curves that are so commonly used in noise assessment actually reflect anything, then that is sound perception.

Using A- and C-weighting curves for predicting auditory hazard implies the assumption that there is a relationship between auditory perception and the risk of hearing injury. We might therefore assume that psychoacoustical sound quality metrics correlate with that risk as well. Using the Sound Quality Analysis Toolbox (SQAT) [11], we computed Perceptual Loudness (PL) in sone [12], Perceptual Sharpness (PS) in acum [13], and Perceptual Roughness (PR) in asper [14]. Note that we used the time-variant (non-stationary) definition in free field and skipped the first 4 ms of the analysis window, i.e., starting 1 ms before the onset. As we seek single predictor values instead of block- or band-wise results, we used averages as well the maximum values as descriptors: $\mathrm{PL}_\mathrm{mean}$, PL_max, $\mathrm{PS}_\mathrm{mean}$, PS_max, $\mathrm{PR}_\mathrm{mean}$, PR_max.

4.4 Acoustic reflex and banded energy

The AHAAH incorporates several non-linear effects that are surely not covered by the acoustical descriptors that have been introduced in this section so far. Two of these are the acoustic reflex and the maximum basilar membrane displacement. Below, we derive very simplified signal processing models for both aspects, in order to obtain acoustical descriptors that may express similar information.

4.4.1 Acoustic reflex

As the activation of the acoustic reflex is a binary decision (triggered when the instantaneous sound pressure passes a threshold of 134 dB) its activation function equals a step function $u_{\mathrm{A}}(t)$ that is 0 before the onset, and 1 afterwards. In the AHAAH model, activation is smoothed by a 1st-order low-pass RC filter with time constant $\tau = 11.7\,\mathrm{ms}$, which we implement as leaky integrator whose output $s_{\mathrm{A}}(t)$ is the smoothed activation function:

$$s_{\mathrm{A}}[n] = (1-\alpha)u_{\mathrm{A}}[n] + \alpha u_{\mathrm{A}}[n-1] \tag{8}$$

$$\text{where} \quad \alpha = e^{-1/(\tau F_{\mathrm{s}})} \tag{9}$$

Once the acoustic reflex is fully activated, its effect can be regarded as a shelving filter that attenuates frequencies below 3 kHz by up to -21 dB (gain $g_{\mathrm{S,min}} = 0.089$) [15, 21]. Assuming that the filter attenuation is directly controlled by $s_{\mathrm{A}}(t)$, the dynamic filter gain becomes:

$$g_{\mathrm{S}}(t) = 1 - (1 - g_{\mathrm{S,min}})\, s_{\mathrm{A}}(t) \tag{10}$$

The applied filter uses a constant cutoff frequency at 3 kHz and a slope of 1, combined with the dynamic gain $g_{\mathrm{S}}(t)$. The application of this simple filter model of the acoustic reflex on a noise measurement is now defined as "unwarned"- or uw-weighting. For the already-included sound energy predictors SEL, ASEL, and CSEL, we add their respective variants $L_{\mathrm{E,uw}}$, $L_{\mathrm{A,E,uw}}$, and $L_{\mathrm{C,E,uw}}$ to the analysis.

4.4.2 Maximum banded sound exposure

Within the AHAAH, the displacement of the basilar membrane is analyzed at 23 discrete locations of equal spacing across its length from the oval window to the round window [16, 15]. These locations are attributed to equally-spaced frequencies on a logarithmic scale, from 11.76 kHz down to 0.38 kHz. A rough approximation of this excitation pattern can be achieved by a gammatone filterbank (GTFB), a widely used model for the auditory filters [17]. For modeling auditory perception, their center frequencies are typically tuned to equal spacing on the ERB-rate scale, with constant bandwidth in parts of the Equivalent Rectangular Bandwidth. In order to match the AHAAH model, we tune them to the same 23 center frequencies, with bandwidths set accordingly so that neighboring bands overlap at their -4 dB cutoff frequency (e.g., as done in [18]). The exposure within the 23 frequency bands b is computed with Z-, A-, and C-weighting, in order to obtain banded exposure levels $L^{\mathrm{b}}_{\mathrm{E}}$, $L^{\mathrm{b}}_{\mathrm{A,E}}$, and $L^{\mathrm{b}}_{\mathrm{C,E}}$, respectively. As the AHAAH evaluates the maximum across locations, we likewise compute the maximum across bands, $L^{\max}_{\mathrm{E}}$, $L^{\max}_{\mathrm{A,E}}$, and $L^{\max}_{\mathrm{C,E}}$, respectively, as acoustical predictors of auditory hazard. In addition, we also consider their uw-weighed variants: $L^{\max}_{\mathrm{E,uw}}$, $L^{\max}_{\mathrm{A,E,uw}}$, and $L^{\max}_{\mathrm{C,E,uw}}$.

5. CORRELATIONS BETWEEN DRC AND ACOUSTICAL DESCRIPTORS

Based on the acoustical descriptors that were derived above, we aimed at explaining differences between DRC and at predicting the respective hazard level by other means. We investigated all possible and meaningful combinations of 1-, 2-, and 3-way linear prediction models (without and with interactions) made from the above descriptors, for predicting the hazard levels of the evaluated DRC. Combinations are considered as meaningful if the predictors are either more robust with regard to technical parameters of the measurement (as of [2]) or more computationally efficient in view of an implementation on embedded platforms. Best fitting models are selected with respect to the Akaike Information Criterion (AIC) in order to avoid overfitting.

5.1 Pfander and Leq

The Pfander level is known for being a good predictor of signal energy, yet avoiding actual integration. The correlation between L_{E} and $L^{\mathrm{Pfander}}_{\mathrm{H}}$ is shown in Fig. 1 for outdoor and indoor recordings, respectively. Outdoors, we observe almost perfect correlation ($L^{\mathrm{Pfander}}_{\mathrm{H}} \approx L_{\mathrm{E}} + 3\,\mathrm{dB}$, $R^2 = 0.989$). If analyzing the difference between target ($L^{\mathrm{Pfander}}_{\mathrm{H}}$) and the linear model based on SEL, the resulting Probability Density Function (PDF) is a superposition of two almost normal distributions (Fig. 2, $R^2 = 0.955$). In Fig. 2 and all following figures, marker colors correspond to weapon categories (Pistols P, Assault Rifles AR, Battle Rifles BR, Sniper Rifles SR, and Explosive E), while marker shapes depict specific models/configurations; filled/unfilled markers represent outdoor/indoor settings, respectively. As the difference between Pfander and Leq primarily concerns diffuseness, the best performing two-way model uses SEL in combination with the DRR ($R^2 = 0.973$), resulting in a PDF more close to normal (Fig.3). Individual weapon configurations now spread along straight lines, which suggests that the majority of the remaining variance is within weapon conditions. The remaining variance could not be explained without the Pfander descriptors $\hat{L}_{\mathrm{p}}$ or T_{A} themselves.

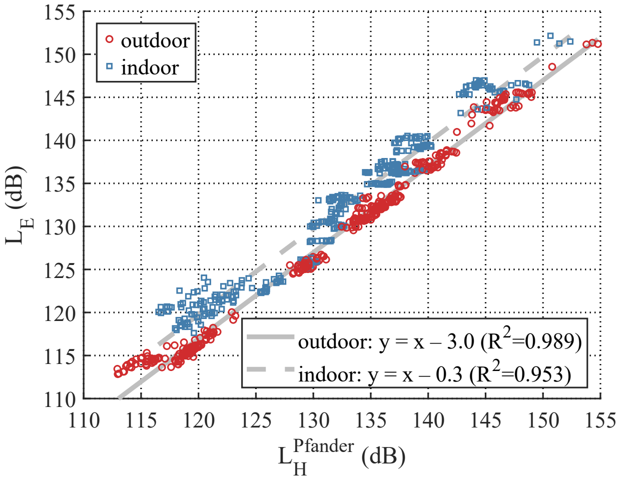

Figure 1. L_{E} as a function of $L_{\mathrm{H}}^{\mathrm{Pfander}}$.

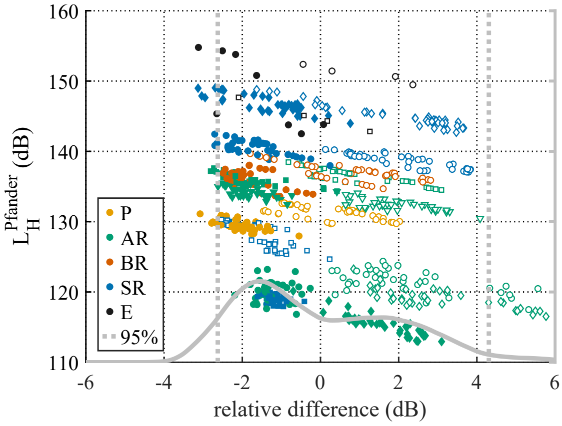

Figure 2. $L_{\mathrm{H}}^{\mathrm{Pfander}}$ predicted L_{E} ($R^2 = 0.955$). Marker coding: color = weapon category, shape = weapon model, filled/unfilled = outdoor/indoor.

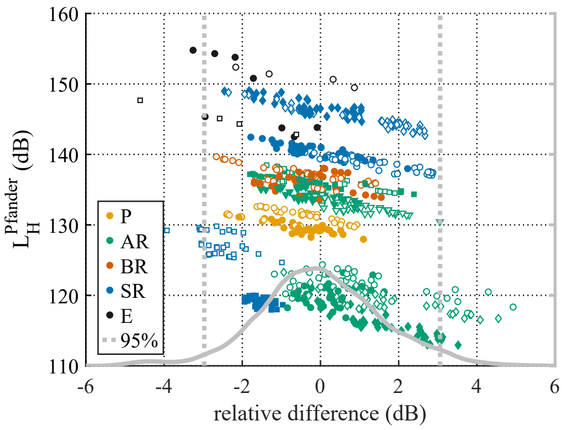

Figure 3. $L_{\mathrm{H}}^{\mathrm{Pfander}}$ predicted by L_{E} and DRR ($R^2 = 0.973$).

5.2 LAeq

The difference between LAeq and Leq is shown in Fig. 4. It follows a characteristic curved shape due to the interplay between A-weighting and noise level. As all tested noises originate from explosions (firearms or explosive charges), the resulting sounds are band-limited, in theory exhibiting a Weber spectrum. Its center frequency decreases with increasing Weber radius, i.e., increasing intensity. Maximum sound energy is thus passed for ASEL ≈ 130 dBA, when A-weighting and Weber spectrum maximally overlap, i.e., when their center frequencies match. The center frequency can be expressed by SC. An interaction between SEL and SC is thus supposed to account for the difference between ASEL and SEL. The best-performing two-way linear model with interactions, however, combined SEL directly with the A-weighted peak, as shown in Fig. 5 ($R^2 = 0.997$). It must be noted that the interaction model of $\hat{L}_{\mathrm{C,p}}$ and k_{A} was almost as good ($R^2 = 0.996$).

5.3 LIAeq

As LIAeq depends on A-duration, it is extremely sensitive to the exact measurement specifications and signal preprocessing, which makes it almost impossible to obtain consistent results [2]. Figure 6 shows the difference between LIAeq and LAeq, thus the effect of A-duration. Note the sniper rifle with silencer (blue squares) for which the A-duration is not meaningful and thus leads to extreme variance. Although a more robust equivalent to T_{A} might be interesting, no useful predictor could be found within the tested acoustical descriptors including their combination.

The best-performing descriptor was $\hat{L}_{\mathrm{p}}$ with only moderate correlation ($R^2 = 0.420$).

5.4 LAeq-Kurtosis

The difference between LAeq-Kurtosis and LAeq (i.e., the contribution of kurtosis adjustment) is shown in Fig. 7. Similar as for the difference between Pfander and Leq, the difference is mainly due to diffuseness. While ASEL alone increases with higher diffuseness due to the added energy of reflections, the resulting difference between indoor and outdoor that is visible in Fig. 7 is effectively minimized through kurtosis adjustment, leading to similar $L_{\mathrm{H}}^{\mathrm{LAeq\text{-}K}}$ indoor and outdoor. $L_{\mathrm{H}}^{\mathrm{LAeq\text{-}K}}$ could be well predicted by

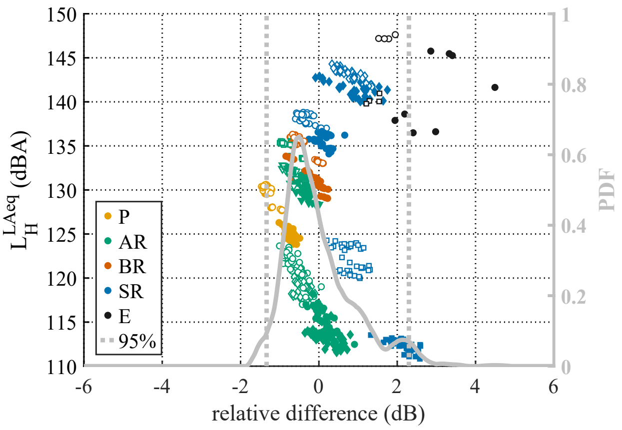

Figure 4. $L_{\mathrm{A,E}}$ predicted by L_{E} ($R^2 = 0.991$).

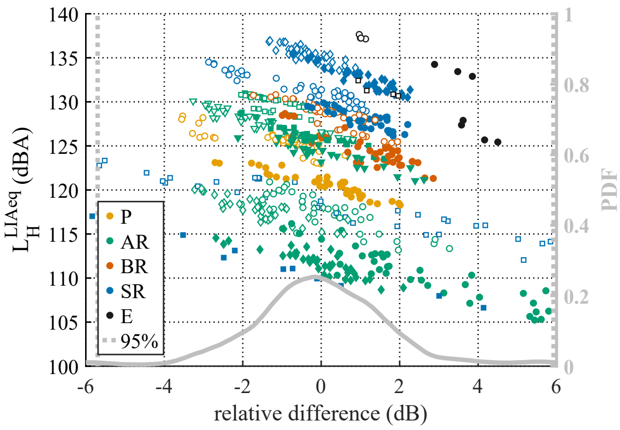

Figure 6. $L_{\mathrm{H}}^{\mathrm{LIAeq}}$ predicted by $L_{\mathrm{A,E}}$ ($R^2 = 0.897$).

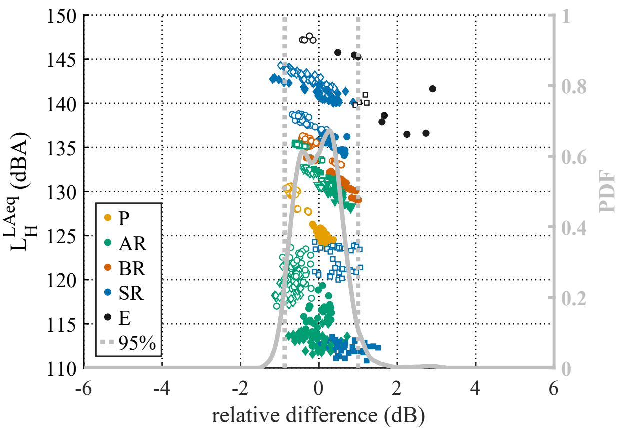

Figure 5. $L_{\mathrm{A,E}}$ predicted by L_{E} and $\hat{L}_{\mathrm{p}}$ (with interaction, $R^2 = 0.997$).

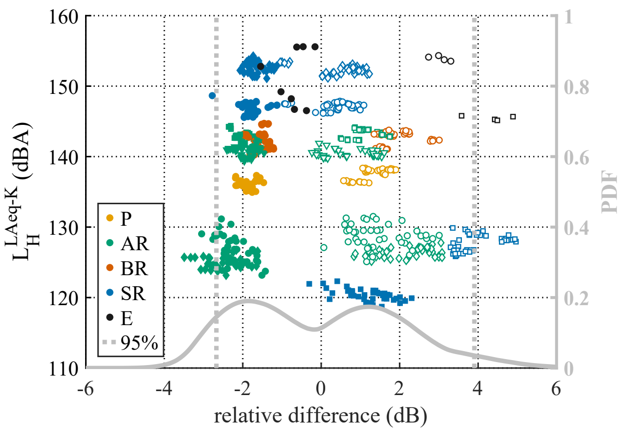

Figure 7. $L_{\mathrm{H}}^{\mathrm{LAeq\text{-}K}}$ predicted by $L_{\mathrm{A,E}}$ ($R^2 = 0.960$).

$\hat{L}_{\mathrm{C,p}}$ alone ($R^2 = 0.986$), as shown in Fig. 8, even better by an interaction model of $\hat{L}_{\mathrm{C,p}}$ and CSEL ($R^2 = 0.998$) or best (in terms of lowest AIC) by $\mathrm{DRR_A}$, $\hat{L}_{\mathrm{A,p}}$ and $L_{\mathrm{A,E}}$ ($R^2 = 0.999$, see Fig. 9). The best single predictor for kurtosis alone was $\mathrm{DRR_A}$ ($R^2 = 0.822$).

5.5 AHAAH

The best-performing single linear predictor of $L_{\mathrm{H}}^{\mathrm{AHA}}$ was the maximum banded ASEL, $L_{\mathrm{A,E}}^{\mathrm{max}}$ (Fig. 10); however, the AHAAH is too complex for being predicted by such a simple signal model and thus only moderate correlation was achieved ($R^2 = 0.640$), on par with ASEL ($R^2 = 0.624$). The unwarned version of banded ASEL with simplified acoustic reflex was no improvement, as the reflections are anyway underrated due to other mechanisms within the AHAAH. The best-fitting two-way model is therefore a linear combination of $L_{\mathrm{A,E}}^{\mathrm{max}}$ in conjunction with DRR, as shown in Fig. 11 ($R^2 = 0.904$).

6. CONCLUSIONS AND OUTLOOK

We compared 6 DRC for impulse noise in terms of their respective prediction of auditory hazard. Comparisons were based on a dataset that covers a majority of the impulsive noise exposure of infantry soldiers.

In order to explain the differences between hazard predictions, we tested different kinds of acoustical descriptors based on the unweighted, A-weighted, and C-weighted sound recording. Classical descriptors included action times, SEL, and peak SPL. Statistical descriptors included kurtosis and DRR. Psychoacoustical descriptors included perceptual loudness, sharpness, and roughness. Additional

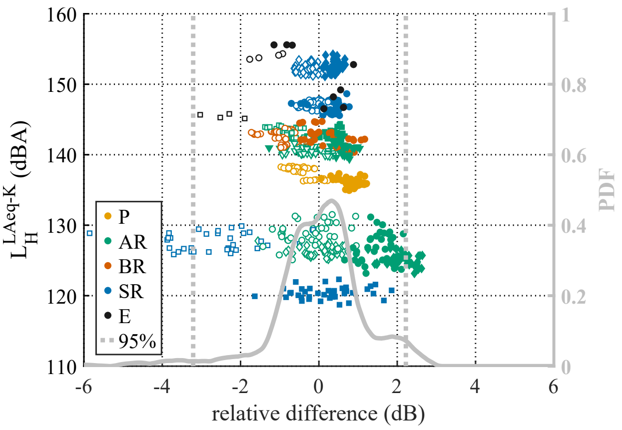

Figure 8. $L_H^{\text{LAeq-K}}$ predicted by $\hat{L}_{\text{C,p}}$ ($R^2 = 0.986$).

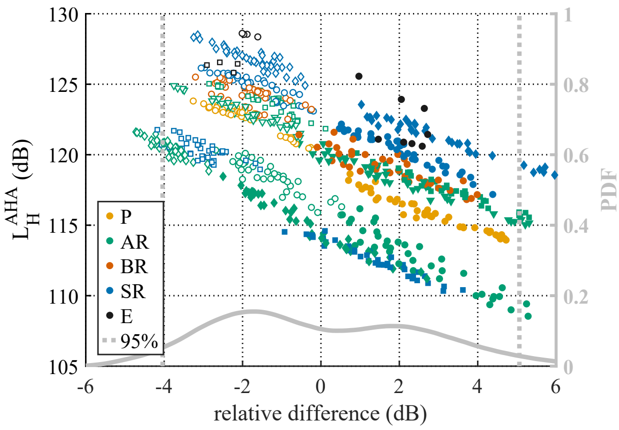

Figure 10. AHAAH (L_H^{AHA}) predicted by $L_{\text{A,E}}^{\text{max}}$ ($R^2 = 0.640$).

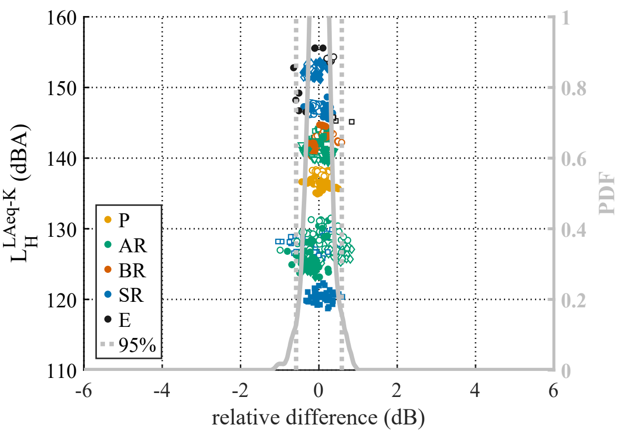

Figure 9. $L_H^{\text{LAeq-K}}$ predicted by DRR_A, $\hat{L}_{\text{A,p}}$, and $L_{\text{A,E}}$ ($R^2 = 0.999$).

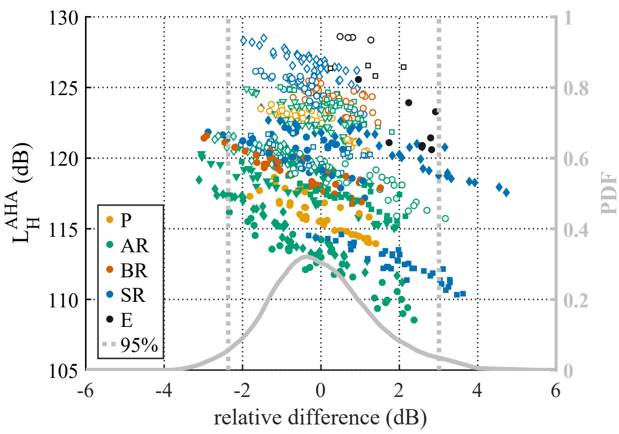

Figure 11. AHAAH (L_H^{AHA}) predicted by $L_{\text{A,E}}^{\text{max}}$ and DRR ($R^2 = 0.904$).

descriptors were derived in order to account for specific characteristics of the AHAAH model. These include a simple filter model of the acoustic reflex as well as a rough approximation of the maximum basilar membrane displacement across fixed positions by taking the maximum exposure across auditory filters.

Most variance between the examined DRC could be explained by linear models of one or multiple descriptors. The difference between Pfander and Leq is mainly due to reflections and thus well expressed by the DRR. The difference between LAeq and Leq, i.e., the effect of A-weighting, could be explained by the interaction between SEL and either peak or SC. LAeq-Kurtosis could be almost perfectly predicted by a combination of C-weighted peak and CSEL. Finally, the auditory hazard predicted by the AHAAH model was best modeled by the maximum of banded ASEL in combination with DRR. The difference between LIAeq and LAeq, i.e., the A-duration, however, could not be sufficiently modeled by any of the tested descriptors. Loudness, sharpness, and roughness did not perform well in predicting the examined DRC. However, this does not exclude a possible correlation with the actual risk of hearing injury, as the examined DRC themselves are insufficiently validated in this concern. We can further conclude that a major aspect of the AHAAH model can be replicated by banded energy. We suppose that similar results could even be obtained from ASEL in $1/3$-octave bands. The simple acoustic reflex model was not useful in this concern, presumably because its effect is concealed by an even stronger effect of diffuseness that is better covered by the DRR. For specific applications such as mobile noise dosimetry, it might be beneficial to use such an alternative computation that is either more robust or less computationally expensive.

The DRR generally proved to be a good predictor of differences between DRC that emerge from diffuseness. As the Pfander criterion exhibits low robustness against measurement specifications due to dependency on peak and zero crossings [2], it might be tempting to replace its computation by a more robust prediction model using SEL and DRR. However, the DRR was found to be equally sensitive as C-duration and is therefore no useful substitute. Other measures of diffuseness should therefore be evaluated in the future. A major shortcoming of this evaluation is the restriction to impulse noise, although some of the DRC were designed for complex noise that includes continuous sound by vehicles or machinery. As the data included only a subset of soldiers' noise exposure, future studies should also include complex noise and heavier weapons in order to draw more general conclusions.

7. ACKNOWLEDGMENTS

This work was done in collaboration with the TA-38 between MoD-NL and MoD-DE on "Hearing damage risk of shooting noise to personnel & underlying damage risk criteria". The cooperation with TNO, WTD91, and Cervus Consult is acknowledged.

8. REFERENCES

[1] F. van der Eerden, E. van Pruissen, and E. Salomons, "Different exposure prediction methods for a wide range of impulsive noises: do they correlate," in *Forum Acusticum, Turin, IT*, 2023.

[2] M. Weger, "Damage risk criteria for impulse noise: How robust are they against measurement specifications?," in *DAGA*, (Copenhagen, DK), 2025.

[3] C. Hudasch, P. Bechtel, K.-W. Hirsch, C. Kleinhenrich, and T. Langenbucher, "Das Pfander-Kriterium im Vergleich zum Gehörgefährdungsindex des AHAAH-Modells," in *DAGA*, (Hannover, DE), 2020.

[4] S. Dantscher and A. Wolff, "Beurteilung der Gehörgefährdung durch Schießlärm: Pfander- oder LAE-Verfahren?," in *DAGA*, (Rostock, DE), 2019.

[5] W. Qiu, W. J. Murphy, and A. Suter, "Kurtosis: a new tool for noise analysis," *Acoust Today*, vol. 16, no. 4, 2020.

[6] "MIL-STD 1474E: Design criteria standard: Noise limits," 2015.

[7] ISL, DGA, and WTD91, "Vorschriften und Richtlinien zur Registrierung und Auswertung von Waffen- und Detonationsknallen," 1995.

[8] F. Pfander, *Das Schalltrauma*. 1994.

[9] G. Goley, W. J. Song, and J. H. Kim, "Kurtosis corrected sound pressure level as a noise metric for risk assessment of occupational noises," *JASA*, vol. 129, no. 3, 2011.

[10] C. Kleinhenrich, P. Bechtel, C. Hudasch, and T. Langenbucher, "Einfluss des Stapediusreflexes auf den Gehörschadensindex des AHAAH-Modells," in *DAGA*, (Hannover, DE), 2020.

[11] G. F. Greco, R. Merino-Martínez, A. Osses, and S. C. Langer, "SQAT: a MATLAB-based toolbox for quantitative sound quality analysis," in *Inter-Noise*, vol. 268, 2023. `https://doi.org/10.5281/zenodo.14641811`.

[12] ISO, "Standard no. 532-1: Acoustics - methods for calculating loudness - part 1: Zwicker method," 2017.

[13] DIN, "Standard no. 45692: Measurement technique for the simulation of the auditory sensation of sharpness," 2009.

[14] P. Daniel and R. Weber, "Psychoacoustical roughness: Implementation of an optimized model," *Acta Acustica united with Acustica*, vol. 83, no. 1, 1997.

[15] G. Price and J. Kalb, "The philosophy, theoretical bases, and implementation of the ahaah model for evaluation of hazard from exposure to intense sounds," *ARL-TR-8333*, 2018.

[16] P. D. Fedele, M. S. Binseel, J. T. Kalb, and G. R. Price, "Using the auditory hazard assessment algorithm for humans (AHAAH) with hearing protection software, release MIL-STD-1474E," *ARL-TR-6748*, 2013.

[17] V. Hohmann, "Frequency analysis and synthesis using a gammatone filterbank," *Acta Acustica united with Acustica*, vol. 88, 2002. `https://github.com/LeoVarnet/Hohmann_Gammatone`.

[18] M. Weger, T. Hermann, and R. Höldrich, "Real-time auditory contrast enhancement," in *ICAD*, 2019.